Role of phase synchronisation in turbulence

Sara Moradi*
Laboratory for Plasma Physics - LPP-ERM/KMS, Royal Military Academy, 1000-Brussels, Belgium

Bogdan Teaca†
Applied Mathematics Research Centre, Coventry University, Coventry CV1 5FB, United Kingdom

Johan Anderson‡
Department of Space, Earth and Enivronment Sciences, Chalmers University of Technology, SE-412 96 Göteborg, Sweden

The role of the phase dynamics in turbulence is investigated. As a demonstration of the importance of the phase dynamics, a simplified system is used, namely the one-dimensional Burgers equation, which is evolved numerically. The system is forced via a known external force, with two components that are added into the evolution equations of the amplitudes and the phase of the Fourier modes, separately. In this way, we are able to control the impact of the force on the dynamics of the phases. In the absence of the direct forcing in the phase equation, it is observed that the phases are not stochastic as assumed in the Random Phase Approximation (RPA) models, and in contrast, the non-linear couplings result in intermittent locking of the phases to $\pm\pi/2$. The impact of the force, applied purely on the phases, is to increase the occurrence of the phase locking events in which the phases of the modes in a wide k range are now locked to $\pm\pi/2$, leading to a change in the dynamics of both phases and amplitudes, with a significant localization of the real space flow structures.

I. INTRODUCTION

In electrically neutral fluids or in plasma flows the presence of nonlinear interactions can lead to the development of turbulence. In general, turbulence is characterized by energetic couplings between different scales of a flow. However, in the context of turbulence driven transport, such as the case of magnetically confined plasmas [1, 2] or the diffusion of cosmic rays [3], typical flow structures are identified by dominant modes and the global turbulent state is approximated by a superposition of linear contributions (waves in general). These theoretical studies consider the amplitudes of the fluctuating quantities, but disregard the dynamics of the phases by using the so-called random-phase approximation (RPA) for which the existence of a Chirikov-like criterion for the onset of wave stochasticity [4, 5] is assumed. In this approximation one assumes that the dynamical amplitudes have a slow variation compared to the rapid change of the phases, which are considered to be distributed uniformly over a 2π interval [1, 2].

The RPA approach is widely used in turbulence transport theory since it has a clear intuitive picture. While it has not been rigorously formulated, there have been attempts in this direction [6]. Its underlying assumption of stochasticity for the phases of Fourier modes in a nonlinearly interacting waves cannot be justified since the phases as well as the amplitudes evolve due to nonlinear interactions that act on the same time scales. Thus, stochastization of phases and amplitudes, if any, occur on the same time scale, see further discussion in Refs. [6, 7].

The correlation of phases due to the existence of nonlinear interactions determines how the spectral energy density, information contained in the amplitude of the Fourier modes, is distributed in real space. This is linked to the intermittent nature of turbulence. Ignoring the phase synchronization, or phase locking between scales, neglects the impact made by coherent structures [8]. Phase dynamics play the crucial role in the self-organization and the formation of coherent structures, as was shown in Ref. [9] for plasma turbulence. The self-organization phenomena is not limited to turbulence, albeit the interest of this work, and is common in other dynamical systems, notable examples being: biological clocks, physiological organisms and chemical reactors [10–19].

In this work, we investigate the role of phase dynamics on turbulent flows. For this analysis, we chose a simple system described by the Burgers equation with an known external force. The prescribed force allows us to control its individual impact on the norm and the phases of the system. In the presence of a force that leaves the phases unaffected, we observe that the phases are not randomized as assumed in the RPA models, and in contrast, the non-linear couplings result in intermittent locking of the phases to $\pm\pi/2$. Employing this force to inject the same power in the system, we can affects the structures developed by the flow through a phase force. Due to the co-evolving and interacting amplitudes and phases, a forcing interacting purely on the phases increases the number of phase locking events, during which the phases are locked to $\pm\pi/2$. In contrast to the stochastically driven oscillator models studied previously [20] the present phase force may be thought of as a strongly coherent force that ultimately change the dynamics of both phases and amplitudes.

In the following we will present the details of our model and the results of the numerical simulations, aiming to elucidate on a series of questions: In which way does a pure phase force affect the structures of the flow? As the dynamics of turbulence is affected and the phase correlations change, how are the spectral energy transfers affected and finally, does a phase force impede or tend to enhance the validity of the RPA

* smoradi@ulb.ac.be
† bogdan.teaca@coventry.ac.uk
‡ anderson.johan@gmail.com

approximation?

II. THE SYSTEM OF INTEREST

A. The Burgers equation

The Burgers equation is a simplified mathematical model for the motion of a viscous compressible flow [21, 22]. In one dimension (x is the spatial coordinate), it reads

$$\partial_t u(x,t) + u(x,t)\partial_x u(x,t) = \nu \partial_{xx} u(x,t) + \delta f(x,t), \quad (1)$$

where u is the fluctuating velocity field, ν is the kinematic viscosity, and $\delta f(x,t)$ is a prescribed external force.

The Fourier representation ($x \rightarrow k$) of the Burgers equation, together with the polar form of the complex fields, i.e.

$$u(k,t) = \psi_k(t) e^{i\theta_k(t)}, \quad (2)$$
$$\delta f(k,t) = f_k(t) e^{i\phi_k(t)}, \quad (3)$$

allows for a decomposition of the dynamics in terms of the norms and the phases as

$$\partial_t[\psi_k(t)e^{i\theta_k(t)}] = -\sum_{k=p+q} i\, p\, \psi_p(t)\psi_q(t) e^{i(\theta_p(t)+\theta_q(t))} - \nu k^2 \psi_k(t) e^{i\theta_k(t)} + f_k e^{i\phi_k(t)}. \quad (4)$$

Hence, we obtain two coupled equations

$$\partial_t \theta_k = -\sum_{k=p+q} \frac{p\psi_p\psi_q}{\psi_k}\cos(\theta_p+\theta_q-\theta_k) + \frac{f_k}{\psi_k}\sin(\phi_k-\theta_k), \quad (5)$$

$$\partial_t \psi_k = +\sum_{k=p+q} p\,\psi_p\psi_q \sin(\theta_p+\theta_q-\theta_k) - \nu k^2 \psi_k + f_k\cos(\phi_k-\theta_k). \quad (6)$$

In the absence of an external force, the dynamics of the phases and the norms are linked by the nonlinear terms (first terms on the left hand side of eqs. 5 and 6), while the viscous term acts solely to damp the amplitude of the Fourier modes. Here, the energy for a scale (denoted by the wavenumber k) is defined as $E(k,t) = \frac{1}{2}|u(k,t)|^2 = \frac{1}{2}\psi_k^2$. The subsequent energy balance equation, obtained from multiplying Eq. (6) by ψ_k, shows that the energy transfer to a scale k, i.e.

$$T(k,t) = \sum_{k=p+q} p\,\psi_k\psi_p\psi_q \sin(\theta_p+\theta_q+\theta_k), \quad (7)$$

is maximum for $\sin(\theta_p+\theta_q+\theta_k) = \pm 1$. For maximal energy transfer and in the absence of forcing, the nonlinear contribution to the time variation of the phases (Eq. 5) is zero and all the phases will be locked (i.e. $\partial_t\theta_k = 0$).

B. The prescribed force

Typically, the external force represents a mechanism to control the energy injection in the system and obtain an energetic steady state. This is highly desirable in the study of dissipative turbulent systems. Here, in a small wavenumber corresponding to the large scales in the system, we choose an *amplitude* force proportional to the velocity,

$$\delta f_A(k,t) = \frac{\epsilon_A}{N_A}\frac{u_k}{|u_k u_k^*|} = \frac{\epsilon_A}{N_A}\frac{1}{\psi_k} e^{i\theta_k(t)}, \quad (8)$$

which allows for the phases of the force to match the phases of the flow for each mode, i.e. $\phi_k = \theta_k$. The number of modes in the forcing range is denoted by N_A and the same amount of energy is injected in each mode. In the steady state, the energy injected by the force balances viscous dissipation ($\epsilon_A \approx \sum_k 2\nu k^2 \psi_k^2$). By construction, we see that $\delta f_A(k)$ does not contribute to the evolution of the phases, i.e. the sin function is zero in Eq. (5). This represents a good test-bed to determine the emerging phase correlations solely due to the nonlinear interactions.

To control the phases in a steady state, a general form of the external force can be used,

$$\delta f(k,t) = \delta f_A(k,t) + \delta f_P(k,t), \quad (9)$$

where we take the *phase* force contribution as

$$\delta f_P(k,t) = \frac{\epsilon_P}{N_P}\frac{u_k}{|u_k u_k^*|} e^{i\pi/2} = \frac{\epsilon_P}{N_P}\frac{1}{\psi_k} e^{i[\theta_k(t)+\pi/2]}. \quad (10)$$

Thus, the $\delta f_P(k)$ contribution to the force does not affect the amplitudes of the modes. Here, the δf_P part to the overall force is acting on the same prescribed wavenumber interval as δf_A (i.e. $N_P = N_A$) and ϵ_P represents a control parameter. Note that the reality condition implies that $f(k)^* = f(-k)$. Directly affecting the evolution of the phases, this force allows to gauge the impact made on structure formation by collective synchronization.

C. Numerical set-up

We solve the equations using a Runge-Kutta 4th order scheme (RK4) with an adaptive time stepping length dt while the sampling time step is $\Delta t = 0.001$. The numerical integration is performed in a periodic domain of length $L = 2\pi$ using N modes (i.e. $k \in [-N/2, N/2]$) and the nonlinear term is computed following a pseudo-spectral method with three-half dealiasing method. In our analysis we use $N = 2048$ modes and consider the initial value $u_k(0) = k^{-2}\exp(i\theta_k)$, where θ_k are taken as random with equal probability between $[0, 2\pi]$. In this study a weak level of Burgers' turbulence is considered, thus allowing for the chosen resolution to be sufficient for the lessons drawn in this work.

Throughout the work, we consider that the force acts in a small wavenumber interval ($|k| \in [3, 7]$) and we take the same energy injection level, i.e. $\epsilon_A = 4 \times 10^{-3}$. The distinction

between the runs analyzed is given by the value of the ϵ_P parameter. In Fig. 1, we plot the energy spectra for these runs. We recover the k^-2 spectral slope in the inertial range, a fact expected for Burgers turbulence. The fact that the system is well resolved is seen by the values of the energy in the highest modes (values that reach machine precision).

III. RESULTS

A. Localization of the flow structures in the real space

We know that the phases and their correlations are important in the development of structures in the flow and are ultimately responsible for the emergence of intermittency. However, how is the phase force employed here affecting the structures of our simple flow?

Fig. 2 shows the computed solution of the Burgers equation, i.e. $u(x,t)$. Here, we have increased the strength of the phase force ϵ_P in three steps, with equal time intervals, from 0 to 2×10^{-3} and subsequently to 4×10^{-3} while maintaining $\epsilon_A = 4\times10^{-3}$ constant throughout the simulation. During the time interval without the phase force i.e. $t = 0 - 3\times10^3$ the turbulent fluctuations are born, and dissipated homogeneously in (x,t) space. By increasing ϵ_P to 2×10^{-3}, the propagating fluctuations are more and more localized in x as well as follow a preferred direction (up-down). This trend is further amplified as the ϵ_P is increased to 4×10^{-3}, where we observe that smaller flow structures rapidly disappear while one structure becomes dominant and propagates as one single traveling wave.

B. Dynamic of the phases

To study the dynamic of the phases we have computed the order parameter shown in Fig. 3 (top). An analytic expression

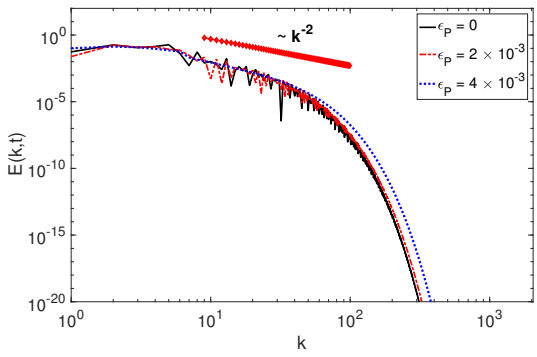

FIG. 1. Typical energy spectra for the steady states. The k^{-2} spectral slope is recovered, a fact expected for Burgers turbulence. Here $\epsilon_A = 4\times10^{-3}$.

for the order parameter,

$$Z(t) = \sum_{k=1}^{N} \frac{1}{N} e^{i\theta_k}, \tag{11}$$

was derived by Kuramoto that describes the quality of the synchronization of the ensemble of phases with $0 \le |Z| \le 1$, where $|Z| = 0$ corresponds to a completely asynchronous state, while $|Z| = 1$ corresponds to a totally synchronous state. Here, to eliminate the numerical noise corresponding to the highest modes (modes unexcited from a physical perspective), we have used a low pass filter with $k_c = 700$ and, for a better illustration of the differences, we have offset the y-axis by 0.3. We observe that in the absence of the phase force, the phases of the fluctuations are asynchronous with the exception of a few occasions where the phases become partially synchronized with peaks in $|Z|$ of $\sim$ 0.8. By applying the phase force, these occurrences become more frequent, and from 3 significant events in the case with no forcing phase, it increases to 11 and 14 significant events in the cases where phase forcing was applied. Also the quality of synchronization has increased strongly reaching peaks of the order of $|Z| \sim 1$ in the last case.

The synchronization of the phases at these occurrences are more clearly observed from the polar view representations of the phases shown in Figs. 3. In the absence of the phase force, at a phase locking event no synchronization between the phases of $|k| \in [1, 20]$ modes is obvious, and the phases of the $|k| \in [21, 121]$ show synchronization to $\pm\pi/2$ with equally divided numbers locked to $\pi/2$ and $-\pi/2$. Here, we find that the quality of the synchronization in the high-k range of $|k| \in [121, 700]$ is not as good. This is induced by the dissipation since as the dissipation dampens the amplitudes, it results in a reduction of the non-linear coupling strength, i.e. $\psi_p\psi_q/\psi_k$, between the phases. Indeed this was tested and we observed that by increasing ν, the range of the stochastic phases expands further into lower k region, whereas by decreasing ν it will recede into higher k's. Thus, the non-linear interactions result in phase locking in the inertial range rather than stochastization of the phases as is commonly assumed in RPA based models. As seen in the two last panels of the polar views in Fig. 3, a force applied exclusively to the phases facilitates phase synchronization allowing for further locking of modes to $\pi/2$ alone. In Ref [6], it is found that synchronization of the phases in wave turbulence occurs over short time intervals as is seen here.

C. Maximization of the energy transfers due to locking

When synchronized, the phases of all three cases shown in the polar representation in Fig. 3, are $\pm\pi/2$ which yield maximum energy transfer for all possible triads, $k+p+q=0$. Because of the wide locked range at the inertia/dissipative scales i.e. mid-to high-k modes, the locking to $\pi/2$ phase (note that due to the reality condition $u^*(k) = u(-k)$ the phase of the negative wave numbers will be locked to $-\pi/2$, not shown in the polar views) should allow for an enhanced

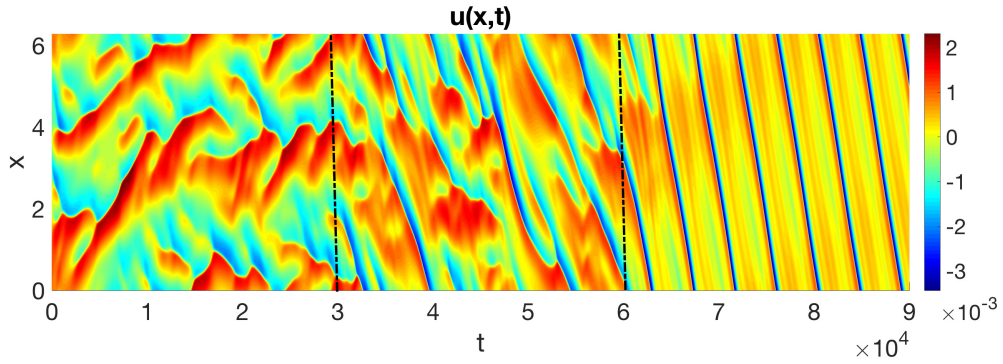

FIG. 2. The solution of Burgers equation, u, as a function of x and t. Here $\epsilon_A = 4 \times 10^{-3}$. The value of ϵ_P is increased in 3 steps denoted by straight lines from 0 to 2×10^{-3} and than to 4×10^{-3}.

removal of the inertia scale energies to the small dissipative scales.

From the definition of the energy transfer, Eq. (7), we see that in general the maximal transfer is obtained for $|\sin(\theta_p + \theta_q + \theta_k)| = 1$ and can be conceptually defined as

$$T^{\max}(k,t) = \sum_{k=p+q} p\,\psi_k\psi_p\psi_q. \tag{12}$$

As we increase the intensity of the phase force, the $\pm\pi/2$ locking events become more frequent and $T(k)$ should tend towards $T^{\max}(k,t)$ more often. To capture this tendency on a simple curve we use the definition provided by Ref. [23] for the intensity of the nonlinear transfers and define the maximal ratio as:

$$M(t) = \frac{\sum_k |T(k)|}{\sum_k |T^{\max}(k)|}. \tag{13}$$

Not only that $M(t)$ tends towards unity during synchronization events, it also allows us to gauge the intensity of the transfers compared to the maximal allowed for the reminder of the time. Figure 4 shows the values of M as function of time for the three considered cases (from top to bottom the value of ϵ_P is increased) during a time window around the locking events shown in polar panels in Fig. 3. Here, also the values of the order parameter $|Z(t)|$ are illustrated for convenience. As can be seen here, in the case of $\epsilon_P = 0$ this ratio, the ratio is around $M \sim 0.5$ and at the moment of strong phase locking, as indicated by the peaks in $|Z(t)|$, it increases significantly to $M \sim 0.85$. Similarly, in the case of $\epsilon_P = 2 \times 10^{-3}$ and $\epsilon_P = 4 \times 10^{-3}$, the moments of phase locking coincides with the increase in the ratio of transfers, M. In the case of $\epsilon_P = 4 \times 10^{-3}$, an oscillatory behaviour is observed with an average of $M \sim 0.55$ and peaks reaching $M \sim 0.85$. This increase in the value of M occurs also at lower value of $|Z(t)|$, where a few subpopulations of the phases are locked at different values e.g. $\pm\pi/2$ and $\pm\pi$, as shown in the polar representations in Fig. 5.

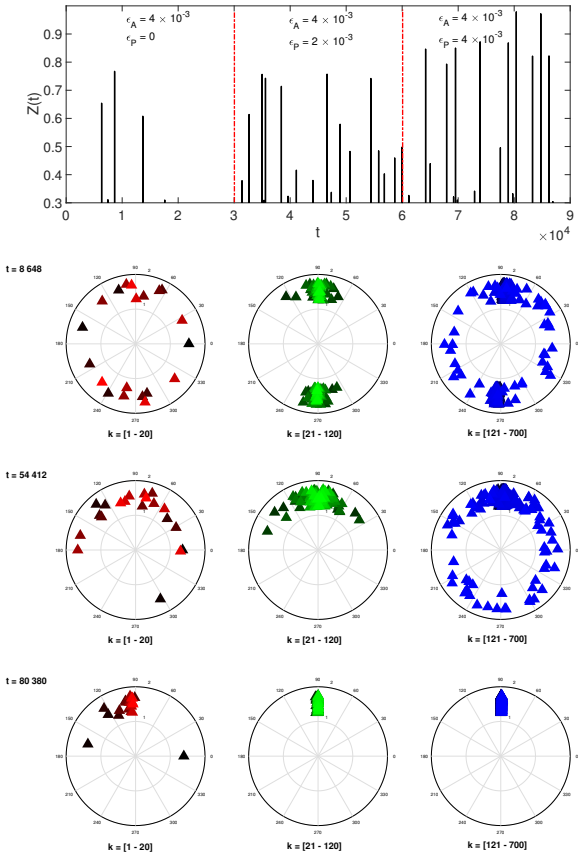

FIG. 3. (top) The order parameter $|Z(t)|$ as function of time, and polar views of the phases at three different time slices corresponding to the highest peaks in $|Z(t)|$ in each case. Here, as the mode number, k, is increased, the colors are varied from darker to lighter shades.

D. Maximization the energy flux towards small scales due to locking

While the energy transfers are important, the energy fluxes offer a better measurement of the energy passing from large

to small scales. The energy flux across a scale k is defined as

$$\Pi(k,t) = \sum_{k'=k}^{\infty} T(k',t), \tag{14}$$

and it is positive for a cascade of energy from large to small scales. Figure 6 shows the time average values of the flux normalized to amplitude forcing strength, $\langle|\Pi|\rangle/\epsilon_A$, as function of mode number k, for the three considered cases. Here, the last 2000 time steps of the simulations, where the steady state conditions are reached, is used for the time averaging. An increase in the values of the averaged flux for the $k = [21-120]$ is observed as the strength of the phase force raised. This is due to the phase force with results in the locked events to become more frequent, as well as spread into a wider range of k's, both in lower-k where the forcing is active, and higher-k where dissipation is stronger. Therefore, during the phase locking events the removal of the large scale energies is further increased and as the number of these events increases, the overall energy of the system is reduced. Indeed, as is shown in Fig. 7, the total energy of the system is reduced as the phase forcing is introduced. For the time interval where the ϵ_P is raised to 4×10^{-3}, the energy oscillates as the wave propagates through the system and finally converges to a finite but lower level as compared to the time period without the phase force. Thus, the observed increase in energy flux of Fig. 6 confirms the enhancement in the transfer of the large scales energy to small scales via phase locking.

A maximal flux, $\Pi^{\max}(k,t)$, can be defined as well by simply employing $T^{\max}(k,t)$ in the definition above to obtain the ratio of the flux to its maximal allowed as

$$M_\Pi(t) = \frac{\sum_k |\Pi(k)|}{\sum_k |\Pi^{\max}(k)|}. \tag{15}$$

Figure 8 shows the values of this ratio i.e. $M_\Pi(t)$, for the three considered cases of Fig. 4. In all the cases, we observe similar patterns in the value of M_Π around the main locking event where M_Π grows from very small values of about $\sim 0.02 - 0.05$ to $\sim 0.3 - 0.6$ with few oscillations around the locking event. This behaviour suggests that there is a build up towards the locking event which also lasts for some time after the actual moment of locking. This build up manifest itself as an increase in the energy flux passed through to the small scales. By increasing the phase force, the time window of the build up becomes shorter, however the pattern remains the same.

IV. CONCLUSION

The phase dynamic in a simple 1D model of Burgers turbulence is examined. External forces which act independently on the amplitudes and phases are introduced. By introducing a special force which only affects the phases, we explored the possibilities of artificially locking the phases.

In real space we observe that in the absence of the phase force the turbulent flows are born, and dissipated homogeneously in (x,t) space. However, by increasing the phase force, the propagating flows are more and more localized in

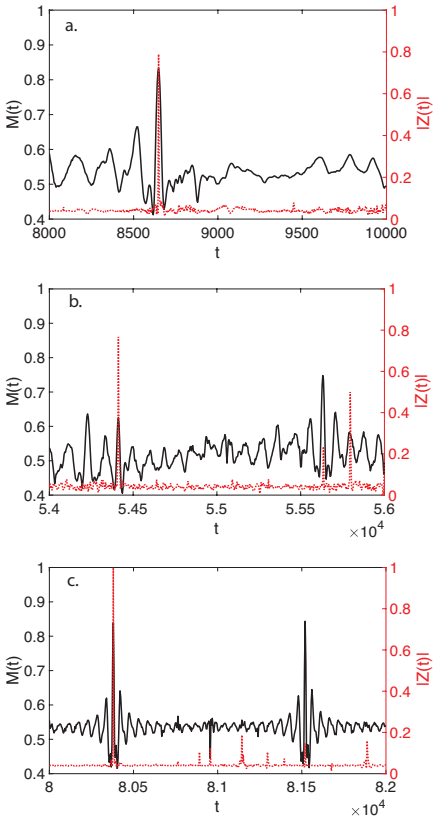

FIG. 4. (On the left y-axes)$M(t)$ as function of time for (a) $\epsilon_P = 0$, (b) $\epsilon_P = 2 \times 10^{-3}$, and (c) $\epsilon_P = 4 \times 10^{-3}$. (On the right y-axes) the order parameter $|Z(t)|$ for the same time window is also shown. Note, the range of the above sums are $|k| \in [21, 700]$.

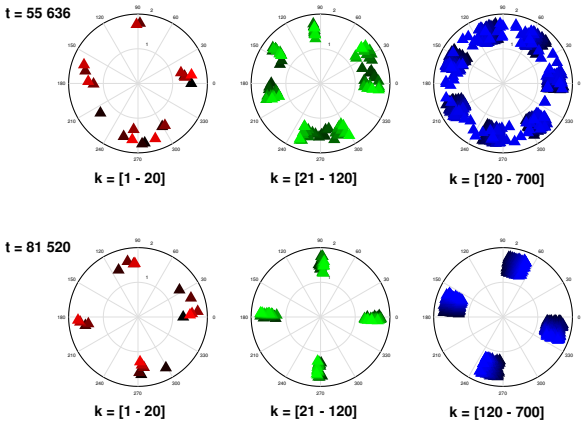

FIG. 5. The polar views of the phases at the time slices corresponding to the second highest peak in $M(t)$ as seen in Fig. 4 (b and c panels respectively). Here, as the mode number, k, is increased, the colors are varied from darker to lighter shades.

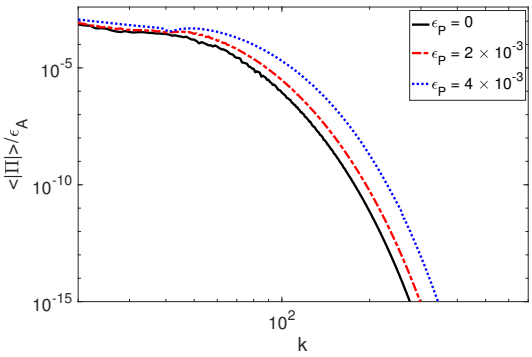

FIG. 6. Time average values of the flux normalized to amplitude forcing strength, $\langle|\Pi|\rangle/\epsilon_A$, as function of mode number k, (black solid line) $\epsilon_P = 0$, (red dashed-dotted line) $\epsilon_P = 2 \times 10^{-3}$, and (blue dotted line) $\epsilon_P = 4 \times 10^{-3}$. The last 2000 time steps of the simulations are used for the computation of the average.

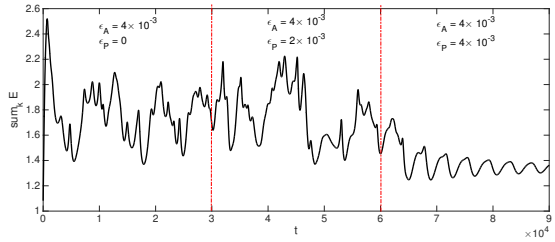

FIG. 7. The total energy ($\sum_k E_k(t)$) as a function of time t with $\epsilon_A = 4 \times 10^{-3}$, and the ϵ_P was increased in 3 steps denoted by straight lines ($0,\ 2 \times 10^{-3},\ 4 \times 10^{-3}$).

x and eventually the smaller flows disappear and one structure becomes dominant and propagates as one single traveling wave.

The observed phase dynamic shows significant departure from the well known RPA assumptions, with phases locking occasionally (but not in the dissipative high-k range). In the well-known Kuramoto [19] non-linear system with two-body interactions of limit cycle oscillators, it was shown that these types of systems are prone to locking if the coupling strength between the two-bodies has passed a threshold. However, the dynamic of the three-body interactions between the phases in the non-linear Burgers' turbulence differs from this simplified picture, and the phases lock intermittently and only in the low to mid-k range. This is due to the k dependence of the coupling strength in the non-linear term which reduces strongly for high-k range due to the dampening effect of the dissipation which does not allow locking of the phases of the small scales. In a locked event, therefore the evolution of the phases (eq. 5) is determined by the contributions of the small scales to the non-linear sum and the forcing which results in an immediate offsetting of the phases from the locked state and the intermittent property of the observed phase locking.

Our results show an increase in the occurrence of the locking events by inclusion of the phase force, thus, further invalidating the RPA assumptions in the studied system.

As the locking increases through the effect of the phase force, we observe a reduction in the total energy. This is attributed to the fact that during the locking events the phases lock to $\pm\pi/2$ which results in maximisation of the transfers, $T(k,t)$. The computed values of the energy flux $\Pi(k,t)$, confirms the increase in the energy flux passed from large scales through to the small scales, as the phase force is raised to higher levels allowing for more locking events to take place. A build up of increased energy flux prior to the moment of locking is observed which also lasts for some time after the locking.

Acknowledgments B. Teaca is partially supported by EPSRC grant No. EP/P02064X/1.

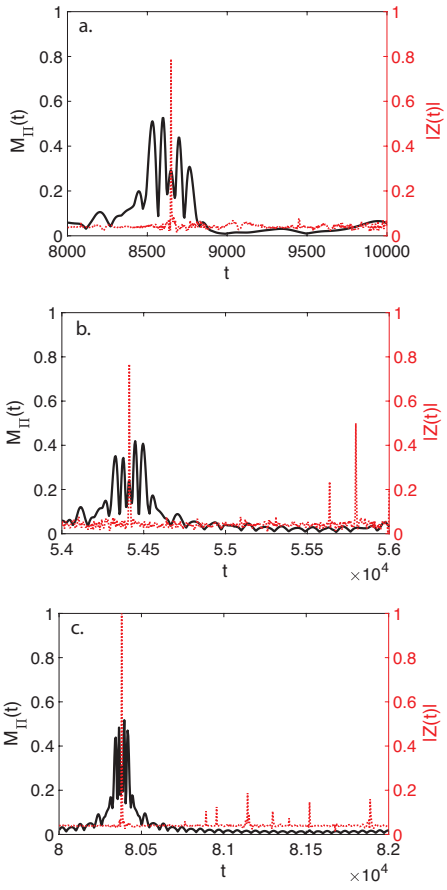

FIG. 8. (On the left y-axes)$M_\Pi(t)$ as function of time for (a) $\epsilon_P = 0$, (b) $\epsilon_P = 2 \times 10^{-3}$, and (c) $\epsilon_P = 4 \times 10^{-3}$. (On the right y-axes) the order parameter $|Z(t)|$ for the same time window is also shown. Note, the range of the above sums are $|k| \in [21, 700]$.

[1] Patrick H. Diamond, Sanae-I. Itoh, Kimitaka Itoh, Modern Plasma Physics: Volume 1, Physical Kinetics of Turbulent Plasmas. *University of Cambridge* (2010).

[2] J. A. Krommes, Fundamental statistical descriptions of plasma turbulence in magnetic fields. *Physics Reports* **360** 1- 352 (2002).

[3] D. Gaggero, Cosmic Ray Diffusion in the Galaxy and Diffuse Gamma Emission, *Springer Theses, DOI:* $10.1007/978-3-642-29949-0\_2$*, Springer-Verlag Berlin Heidelberg* (2012).

[4] G. M. Zaslavski and R. Z. Sagdeev, *Limits of statistical description of a nonlinear wave field*, Zh. Eksp. Teor. Fiz. **52** 1081 [Sov. Phys. JETP **25** 718 (1967)] (1967).

[5] V. E. Zakharov, *Statistical descriptions and plasma physics* In: A. A. Galeev and R. N. Sudan (Eds.), Handbook of Plasma Physics, Vol. 2. North-Holland, Amsterdam, p. 3 (Chapter 5.1) 1984.

[6] Yeontaek Choi, Yuri V. Lvov, Sergey Nazarenko, *Physica D* **201** 121–149 (2005).

[7] S. Nazarenko, Lecture Notes in Physics 825, Wave turbulence. *Springer DOI: 10/1007/978-3-642-15942-8.* Volume 825 (2011).

[8] H. Branover and Y. Unger, Progress in turbulence research, *American Institute of Aeronautics and Astronautics, Inc. Washington DC.* Volume 162 (1993).

[9] Z. B. Guo and P. H. Diamond, *Phys. Rev. Let.* **114** 145002 (2015).

[10] A. T. Winfree, The Geometry of Biological Time, *Springer, New York* (1980).

[11] H. Daido, *Prog. Theor. Phys.* **77** 622 (1987).

[12] H. Daido, *Phys. Rev. Lett.* **68** 1073 (1992).

[13] J. D. Crawford, *J. Stat. Phys.* **74** 1047 (1994).

[14] H. Daido, *Phys. Rev. E* **61** 2145 (2000).

[15] S. H. Strogatz, *Physica D* **143** pp 1-20 (2000).

[16] H. Hong and S. H. Strogatz, *Phys. Rev. Lett.* **106** 054102 (2011).

[17] B. Sonnenschein and L. Schimansky-Geier, *Phys. Rev. E* **88** 052111 (2013).

[18] E. Kim and P. Diamond, *Phys. Plasmas* **10** 1698 (2003).

[19] Y. Kuramoto, Chemical Oscillations, Waves and Turbulence, *Springer, Berlin* (1984).

[20] S. Moradi and J. Andersson, *Phys. Plasmas* **23** 052310 (2016).

[21] G.B. Whitham, Linear and Nonlinear Waves, *John Wiley Sons* (1974).

[22] Sharath S. Girimaji and Ye Zhou, Spectrum and Energy transfer in steady Burgers turbulence. *NASA Contractor Report 195047 ICASE Report No. 95-13* (1995).

[23] B. Teaca, F. Jenko and D. Told, *New J. Phys.* **19** 045001 (2017).